

Enhanced performance of a green inorganic-based passive film on the batch hot-dip galvanized steel by organic additives

*Yongfeng Long**, *Changsheng Liu**, *Sunjuan Peng*

College of Materials Science and Engineering, Northeastern University, Shenyang 113024, China

*E-mail: yongyeyongfeng@126.com, cslu@mail.neu.edu.cn

Received: 23 October 2019 / Accepted: 19 December 2019 / Published: 10 February 2020

Till date, there are extremely limited reports on the green passivation technologies for the batch hot-dip galvanization. Herein, an environmental-friendly passivation route for batch hot-dip galvanization using reactive inorganic salts along with little organic substances, such as silane and rust-proof wax emulsion, as additives was developed. The effect of presence of organic additives on the performance and formation process of the inorganic-based passive film were studied via neutral salt spray test, surface contact angle measurement, electrochemical tests, scanning electron microscopy, and energy dispersive X-ray spectroscopy. The results show that the additives significantly enhanced the corrosion resistance and reduced surface tension of the passive film. The additives did not participate in the reaction with zinc layer and no clear change in overall morphology of passive film was observed. However, a concentration of additives was formed on the film's surface to prevent the penetration of corrosive medium into the film. Overall, the organic additives even at low amounts could dramatically improve the comprehensive performance of the passive film, which would be useful for industrial applications in a low-cost and environmental-friendly way.

Keywords: Batch hot-dip galvanization; Environmental-friendly passivation; Organic additives; Enhancement of performance.

1. INTRODUCTION

Hot-dip galvanization is often used to prepare typical anodic protective coatings on steels, and is divided into two representative processes namely continuous and batch. Passivation treatment is in general required to improve the anti-rust ability of the zinc coatings. The passivation solutions for dealing with batch hot-dip galvanized steel primarily contain hexavalent-chromate, which causes serious pollution throughout the complete process of manufacture, circulation and use of products and seriously endangers the human health and environment. Therefore, the development of an environmental-friendly passivation process for batch hot-dip galvanization is highly desirable.

In last decades, the studies on chromate-free (also named as green) passivation technologies for zinc coating have mainly been focused on hot-dip galvanized steel strip. To this end, several classical organic chemicals, including resin, silane, and wax emulsion have been used as main film-forming substances for passive the film. Small amounts of inorganic ingredients such as oxyacid salts of molybdate, zirconium, or vanadium-titanium and nano-SiO₂ sol have been added as corrosion inhibitors to enhance the film's performance [1-9]. However, this organic-based passivation technology has clear limitations for the passivation-treatment of batch hot-dip galvanized steel. Firstly, the non-planar structure of the workpiece subjected to batch galvanization, such as steel pipe, angle steel, metal tower, hardware, and other metal products with complex shapes, affects the thickness and uniformity of the acquired passive film. Furthermore, some common organics of passivation solution (such as resin and silane) easily accumulate in blind holes, chamfers, grooves, and arcs of the workpiece, making the cross-linking and curing difficult in order to form qualified passive films. Secondly, the drying and curing times of the obtained wet passivation film require high energy consumption due to large thickness of the workpiece. Finally, the low cleanliness of the workpiece surface reduces the adhesion and anticorrosive performance of the obtained passive film.

To address these issues, herein, for the first time, a green passivation technology has been successfully developed for the anti-rust treatment of the batch hot-dip galvanized steels. To achieve excellent corrosion resistance, large amounts of reactive inorganic substances (>90 Wt.% of effective ingredients) were employed to strengthen the inorganic conversion film by effective reaction with zinc layer and small amounts (<5 Wt.% of effective ingredients) of special organics were added as additives to improve the film's performance. This is because most chromate-free passivation technologies with only inorganic salts have inadequate protective abilities as they usually require long periods of neutral salt spray testing (above 72 h) [10-21].

In this study, effects of the organic additives on the formation and primary properties of obtained passive films were investigated using various analytical methods and the films were prepared by the developed environmental-friendly passivation technology for the batch hot-dip galvanization. The results suggest that little amounts of organic additives significantly enhanced the corrosion resistance and reduced surface tension of the inorganic-based passive film, meanwhile, the additives did not participate in the reaction with zinc layer and not clearly change the overall morphology of the film, but rather concentrated on its surface to prevent penetration of the corrosive medium. Therefore, a novel green passivation technology for batch hot-dip galvanization was successfully developed by using low amounts of the organic additives.

2. EXPERIMENTAL

2.1 Preparation of passivation solutions and passivation-treated samples

• Preparation of passivation solutions

Two passivation solutions named as solution 1 and solution 2 were prepared by industrial grade chemicals and deionized water (DI water). The contents of solution 1 were all reactive inorganics, and the solution 2 was prepared by adding a little special organic additives (~ 0.6 g/l silane KH-560 and ~

0.3 g/l antirust wax emulsion E360) to solution 1. The detailed chemical compositions of two passivation solutions are presented in Table 1.

• *Preparation of passivation-treated samples*

The substrates employed for the passivation-treated samples were galvanized square pipes (50 mm×50 mm×80 mm). The samples were firstly cleaned with water-based degreaser (1% NaCO₃, 0.1% surfactants, and remaining DI water), then rinsed with deionized water, and then, dried using hot air. The three passivation-treated samples were prepared by immersing the substrates into different solutions at ~25°C for 60s, and then, dried till the surface temperature of each specimen was ~70°C. The obtained samples prepared in different ways were denoted as: sample 1 (galvanized pipe passivated with pure water), sample 2 (galvanized pipe passivated with solution 1), and sample 3 (galvanized pipe passivated with solution 2), respectively.

Table 1. Detailed chemical compositions of solution 1 and solution 2

Composition	Solution 1	Solution 2	Manufacturer
(NH ₄) ₆ Mo ₇ O ₂₄	50 g/l	50 g/l	Taizhou BEST Molybdenum Goods Co., Ltd. China
NH ₄ H ₂ PO ₄	80 g/l	80 g/l	Suzhou Tenghao chemical technology Co., Ltd. China
NH ₄ VO ₃	20 g/l	20 g/l	Suzhou Kangshuo chemical Co., Ltd. China
Co(NO ₃) ₂	5 g/l	5 g/l	Shanghai Liangren chemical Co., Ltd. China
KH-560	-	0.6 g/l	Qingdao Hengda chemical technology Co., Ltd. China
E360	-	0.3 g/l	H.J.UNKEL Co., Ltd. China
DI. Water	remaining	Remaining	-

2.2 *Effects of additives on performance of passivation-treated samples*

2.2.1 *Corrosion resistance*

• *Neutral salt spray test (NSST)*

The NSST was performed on samples 1, 2, and 3 as per GB/T2423.17 standard in a cyclic chamber with model number SYW-60 (XIANGFENG Laboratory Apparatus Co., Ltd. Shanghai, China). In the testing, the salt fog was composed of 5 wt % NaCl solution with pH ~7.0, and the temperature of fog was maintained at 35 ± 2°C. The appearing time and area of rust on sample's surface were recorded at different testing times.

• *Electrochemical tests*

The open-circuit potential vs. time curves (OCP vs. time curve), potentiodynamic polarization (PP) curves, and electrochemical impedance spectroscopy (EIS) profiles were measured on an electrochemic workstation (Wuhan Corrtest Instruments Co., Ltd. China) connected to classic three-electrode cell containing 3.5wt% NaCl solution with pH ~5.0. The passivation-treated sample was used as working electrode, platinum as auxiliary electrode, and saturated calomel as reference electrode. The measuring time for OCP vs. time curve measurements was set to 1200s. The PP curves were acquired at potentials ranging from -1750 mV to 250 mV at the sweeping rate of 1 mV/s. The frequency for EIS tests ranged from 10 mHz to 10 KHz and the amplitude was set to 5 mV under the OCP.

2.2.2 Contact angle measurements

The contact angle measurements of NaCl solution on the surface of samples 2 and 3 were conducted on a professional Contact Angle Measuring Instrument (Shang hai FangRui Instrument Co., Ltd, China). The detailed procedure of measurement was performed as follows. Firstly a sessile drop of 3.5 wt % NaCl solution with pH ~7.0 was deposited on the passivation-treated sample's surface. Then, the image of drop was fixed after its profile was stable and axis symmetrical, and the contact angle value was calculated using a self-attached program to the instrument.

2.2.3 Morphological and composition analysis

The surface morphology of samples 1, 2, and 3 were observed under scanning electron microscopy (SEM) ZEISS EVO18, Germany. The composition of passive film on the passivation-treated samples' surface was determined via energy-dispersive X-ray spectroscopy (EDX) equipped with SEM.

2.3 Effects of additives on film-forming process in passivation solutions

2.3.1 OCP vs. time curve for film-formation in solutions 1 and 2

In a typical three-electrode cell connected to the electrochemistry workstation ((Wuhan Corrtest Instruments Co., Ltd. China), the substrates of galvanized pipes were used as the working electrode, platinum as the auxiliary electrode, and saturated calomel as the reference electrode, with solutions 1 and 2 as electrolytes. The OCP vs. time curves for film-formation on substrate immersed in both solutions were recorded for 1800 s at room temperature. Obtained curves were used to compare the film-formation performances under different passivation solutions with and without additives.

2.3.2 morphological and compositional change during film-forming in solution 2

Passive films deposited on substrates were prepared in solution 2 under different passivation times of 30 , 60 , 120 , 180 , 240, and 300 seconds. The surface morphologies and compositions change of obtained films were then compared by SEM (ZEISS EVO18, Germany) and its coupled EDX, respectively. The influence of additives on morphologies and compositions during the film-formation were then analyzed effectively.

3. RESULTS AND DISCUSSION

3.1. Effects of additives on the corrosion resistance of obtained passive films

3.1.1. NSST

As a common accelerated corrosion method to simulate the process in real environmental condition, NSST is usually adopted to evaluate the protective property of a passive film [22, 23]. The rust area at different testing time of passivation-treated samples at different testing times is listed in Table 2 in order to make a qualitative comparison. The surface appearance of samples after testing is shown in Fig. 1. By analysing the corrosion datas and status of samples, severe rust (area > 80%) was observed on sample 1 after 24 h. Slight corrosion (area ~ 5%) appeared on sample 2 after 48 h, then, as

the test time increased, the rust area gradually expanded (~ 10% after 72 h and >50% after 96 h). Little rust (area ~1%) also appeared on sample 3 after 72 h, and the area expanded to ~5% after 96 h.

Hence, the results suggest that the passivation-treated samples without and with organic additives all had clear protective performance. Moreover, compared with the sample without organic additives, the corrosion resistance of the ones with organic additives significantly improved. In other words, the existence of organic additives in the obtained passive film can effectively enhance its resistance to salt mist corrosion.

Table 2. Rust area of different passivation-treated samples in NSST after different testing times (%)

	24 h	48 h	72 h	96 h
Sample 1	>80	-	-	-
Sample 2	-	about 5	about 10	>50
Sample 3	-	-	about 1	<5

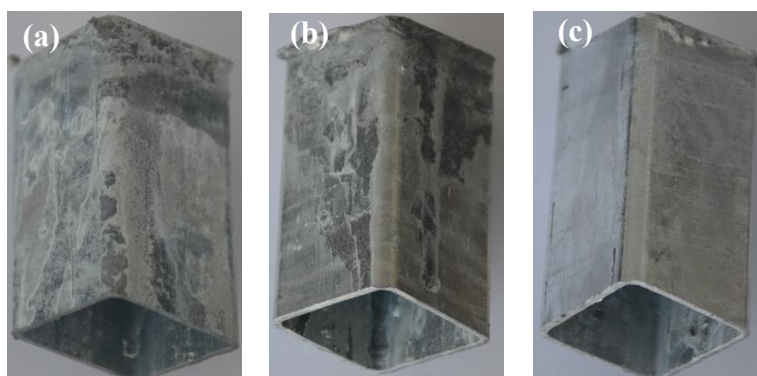


Figure 1. Corrosion status of different passivation-treated samples in NSST after different testing times. (a) sample1 after 24 h, (b) sample2 after 96 h, and (c) sample3 after 96 h.

3.1.2. Electrochemical behaviors of obtained passive films in 3.5 % NaCl (pH=5) solution

3.1.2.1. OCP vs. time curves

Fig. 2 presents the OCP vs. time curves of samples 1, 2, and 3 in 3.5% NaCl (pH=5) solution, in which the obtained passive films were dissolved and destroyed [24, 25]. There were remarkable difference in three transient curves. The initial open circuit potentials, E_{OC} , of sample 2 (~ -1.078 V) and sample 3 (~ -1.027 V) were higher than that of sample 1 (~ -1.105 V), in addition, that of sample 3 was clearly higher than sample 2. As time increased, the curves of each sample depicted different trends. The potential of sample 1 stabilized at about -1.108V after a slight decrease for 60 s. The potential of sample 2 slowly reduced to ~ -1.088V for 800 s, while that of sample 3 extremely slowly reduced to ~ -1.054V for 1000 s before stabilizing. Moreover, the E_{OC} decreasing rate of the sample 3 was less than that of

sample 2. The final stable potential of the sample 3 was also clearly higher than those of the other two samples. Thus, the initial potentials of samples 2 and 3 were positive when compared to sample 1, making the first two as protective films. On the other hand, the passive films on the surface of samples 2 and 3 also dissolved gradually during the test. The dissolution rate and degree of sample 3 were significantly lower than those of the sample 2.

As can be clearly observed in the curves, the addition of organic additives enhanced the stability and corrosion resistance of the obtained passive film under corrosive environments.

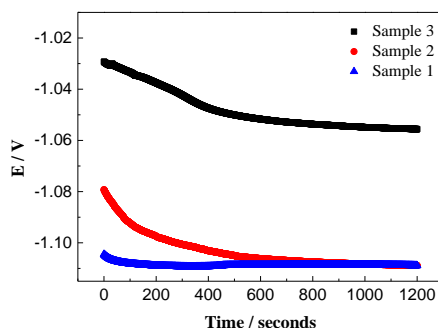


Figure 2. OCP vs. time curves of different passivation-treated samples in 3.5% NaCl solution at pH=5.

3.1.2.2. PP curves

Fig. 3 exhibits the PP curves of passivation-treated samples in 3.5% NaCl (pH = 5) solution. The polarization curves of samples 2 and 3 were different from that of sample 1 in both shape and position. Clear passive platforms were observed in the anodic section of the curves for the two samples 2 and 3. Which also moved to the bottom right side when compared to that of sample 1. Therefore, the corrosion process of passive films was controlled by the anode reactions [26].

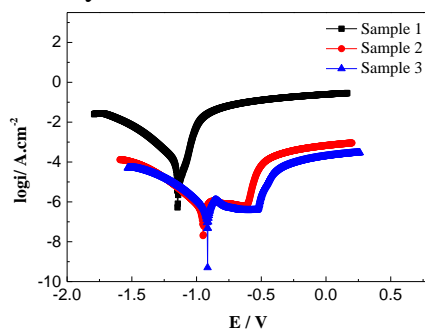


Figure 3. PP curves of different passivation-treated samples in 3.5 % NaCl solution at pH = 5.

Table 3 shows the fitted parameters of PP curves for the three samples. The i_{corr} of samples 2 and 3 were significantly smaller as compared to that for sample 1. The i_{corr} of sample 3 was much smaller than that of sample 2. Also, the E_{corr} of samples 2 and 3 were clearly more positive than that of the unpassivated one (sample 1). The R_p of samples 2 and 3 were significantly larger than that of sample 1, while that of sample 3 was much larger than the value of sample 2. In summary, the results of PP curves

indicat the corrosion resistance of the obtained passive film was effectively improved after organic-adding [27, 28, 29].

Table 3. Fitted parameters from the PP curves of different passivation-treated samples.

	i_{corr} ($\mu A/cm^2$)	E_{corr} (V)	R_p (Ω/cm^2)
Sample 1	4.77×10^0	-1.14	3.76×10^3
Sample 2	3.40×10^{-1}	-0.949	5.39×10^3
Sample 3	6.92×10^{-2}	-0.916	2.60×10^4

3.1.2.3 EIS analysis

Fig. 4 illustrates the EIS results of three passivation-treated samples, wherein Nyquist plots are presents in Fig. 4 (a) and Bode plots in Fig. 4 (b) and Fig. 4 (c). The semicircle diameter in Nyquist plot and low-frequency modulus in Bode plot directly reflect the protective performance of a passive film, wherein a larger value represents better corrosive resistance [30]. As shown in the figures, the semicircle diameters of samples 2 and 3 were far larger than that of sample 1, while, the diameter of sample 3 was larger than that of sample 2. At low frequency zone of Bode modulus plots, the impedance of sample 3 was maximum, followed by that of sample 2, and then, sample 1.

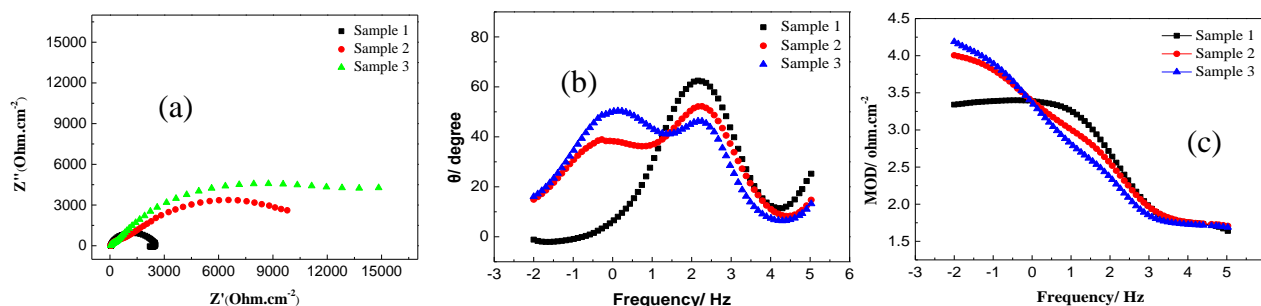


Figure 4. EIS results of different passivation-treated samples in 3.5 % NaCl solution at pH = 5. (a) Nyquist plots, (b) Bode phase plots, (c). Bode modulus plots.

There were two peaks (corresponding to two time constants distributed in the low and high frequency zones, respectively) for samples 2 and 3, but only one (corresponding to time constant distributed in the high frequency zone) for sample 1. The time constant in low frequency zone presents the transfer impedance-resistance of the interface double layer, while that in high frequency zone was linked to impedance-resistance of the passive film on the surface [31,32,33]. As per the results of EIS diagrams, there were clear protective layers named passive films on the surface of samples 2 and 3, and the anti-rust performance of sample 3 was remarkably better than that of sample 2 [34, 35, 36].

To further explain the EIS data, the corresponding equivalent electric circuits (EEC) of different samples during the corrosion process are shown in Fig. 5. Fig. 5 (a) represents the typical EEC model of R(RQ) for an active metal without protective film (sample 1), while Fig. 5 (b) is the classic model of R(Q(R(RQ))) for the substrate with deposition of protective film. There are five components in EEC of

Fig. 5. The resistor R_s represents the solution resistance. The two constant phase elements are CPE1 and CPE2, respectively. The resistance of ionic current through the pore is noted as R_p , and the last part, R_c , is the charge transfer resistance of the passive films.

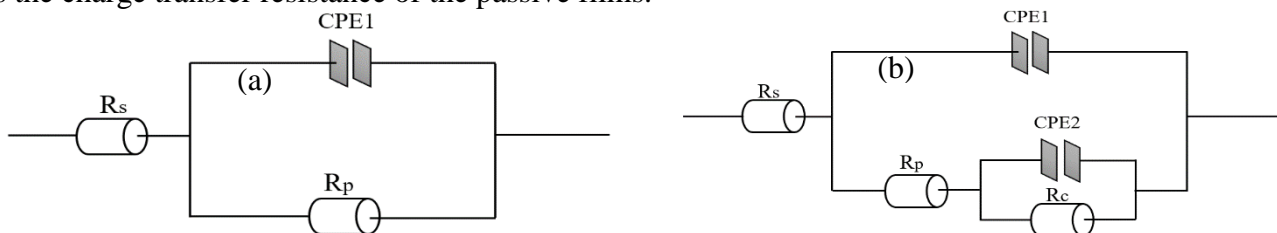


Figure 5. Equivalent electrical circuits fitted by EIS data of different samples. (a) model of sample 1, (b) model of samples 2 and 3.

All the fitted parameters from the EIS programs of different passivation samples are presented in Table 4. The R_p values of sample 3 was the biggest, followed by those of sample 2 and then sample 1. This difference clearly indicates the porosity decrease in the order sample 1, sample 2, and then, sample 3, which agrees with the SEM results presents in Fig. 6. The CPE1 values also decreased in the same order. The R_c and CPE2 values of sample 3 were larger than those of sample 2, indicating that sample 3 had a better anti-corrosion ability. The n values further reflect their surface characteristics, when it being greater than 0.5, indicate that the sample's surface had good uniformity and the fitted parameters were also reliable.

Table 4. Fitted parameters from the EIS data of different passivation samples

	R_s ($\Omega.cm^2$)	R_p ($\Omega.cm^2$)	R_c ($\Omega.cm^2$)	CPE1 ($\Omega^{-1}.cm^{-2}.s^n$)	CPE1-n	CPE2 ($\Omega^{-1}.cm^{-2}.s^n$)	CPE2-n
Sample 1	52.84	459.5	-	8.42×10^{-6}	0.85	-	-
Sample 2	53.07	1028	1.22×10^4	1.44×10^{-4}	0.62	1.54×10^{-5}	0.79
Sample 3	51.74	2425	1.43×10^4	1.05×10^{-4}	0.69	1.72×10^{-5}	0.85

To summarize, the performances of all above presented evaluation methods (in section 3.1) on protective abilities of passivation-treated samples were consistent, suggesting that the existence of organic additives in passive film can significantly enhance its corrosive resistance.

3.2. Effect of additives on the contact angle of NaCl solution on the obtained passive films' surface

Fig. 6 illustrates the results of contact angle measurements of 3.5% NaCl solution (pH = 7) on surface of samples 2 and 3. The contact angle value reflected hydrophobicity of the obtained passive film, wherein a larger reflects higher hydrophobicity and its resistance to corrosive environment is also stronger [37, 38, 39].

As per datas in Fig. 6, the contact angle value of sample 3 (70°) was significantly larger than that of sample 2 (40°). Hence, organic-adding in the passive film could improve its hydrophobicity, and then, prevent agglomeration of the corrosive medium on the surface, and in process, delay the corrosion process.

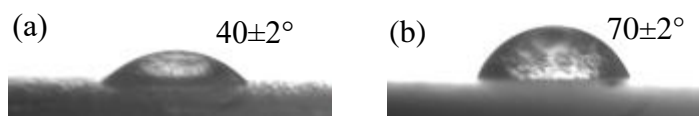


Figure 6. Contact angle of NaCl solution on the surface of different passivation-treated samples. (a) sample 2, (b) sample 3.

The results of contact angle measurement for passive films further confirm the conclusion of above study (section 3.1) on corrosion resistance for passivation-treated samples. Sample 3 (with organic additives) had higher hydrophobicity than sample 2, hence, it had better protective performance.

3.3. Effect on the morphology and composition of passive films

Fig. 7 provides the SEM surface morphologies of different passivation-treated samples. The micrograph of sample 1 shows typical angular and rock-stacked zinc crystal layer. The micrograph of the samples 2 and 3 presents finer sponge-like conversion coatings with certain density grain boundary and invisible rock-like zinc grains. Moreover, numerous gaps, pits, and pores were observed on surface of sample 2, and they were filled or covered by cloud-like matter on the sample 3.

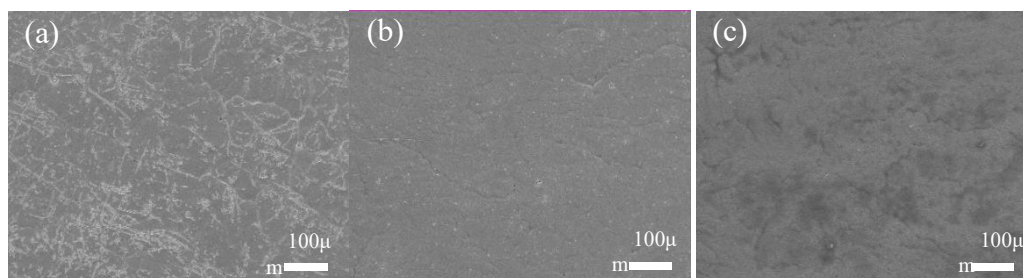


Figure 7. SEM micrograph of surface of different passivation-treated samples. (a) sample 1, (b) sample 2, and (c) sample 3.

Fig. 8 shows the EDX detection of different passive films and their elemental analysis is presented in Table 5. After comparing the elements distribution, in addition to silicon, similar elements and contents were found from the results for samples 2 and 3. Thus, the surface morphology and composition of the passive film were almost not affected by the organic-addition.

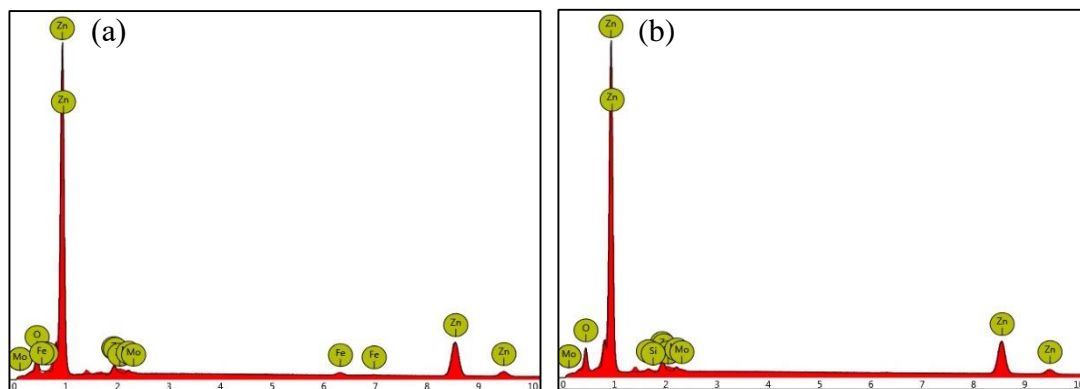


Figure 8. EDX spectra of surface of different passivation-treated samples. (a) sample 2 and (b) sample 3.

Table 5. Elemental analysis from the EDX spectra of different passivation-treated samples (mass %).

	Zn	O	Mo	P	V	Si
Sample 2	54.29	23.15	2.02	1.88	0.08	0
Sample 3	53.96	22.97	1.98	1.83	0.06	0.61

3.4. Effects of additives on the film-formation process in passivation solutions

3.4.1 OCP vs. time curves of substrates in solutions 1 and 2

Fig. 9 presents the OCP vs. time curves of galvanized substrates in passivation solutions with and without organic additives during a period of 30 min in which the passive films formed [40]. The trend of two curves was basically similar, but there were also some differences. At the start of immersion, the E_{OC} of galvanized substrate in solution 2 (~ -1.0745 V) was higher than that in solution 1 (~ -1.083 V). This difference may be due to the addition of organic additives, which reduced pH of the passivation solution [41]. As the test proceeded, the E_{OC} of both systems became positive at different rates. In solution 1, the potential increased rapidly from -1.0830 V to a pole value within 300 s, and then, became stable. In solution 2, the potential rose rapidly within 60 s from -1.0745 V to -1.0685 V before slowly reaching a steady-state value (~ -1.0660 V). We infer that the passive film deposition on the substrate was almost completed within 60 s in solution 2 and 300 s in solution 1. In addition, the stable E_{OC} observed in solution 1 was more negative than that in solution 2. This indicates that growth rate of passive film in solution 2 might be faster than that in solution 1. Furthermore, the corrosion resistance of passive film in solution 2 was also better than that in solution 1 [42,43]. Overall, the organic additives showed good modification effect on growth of the passive film.

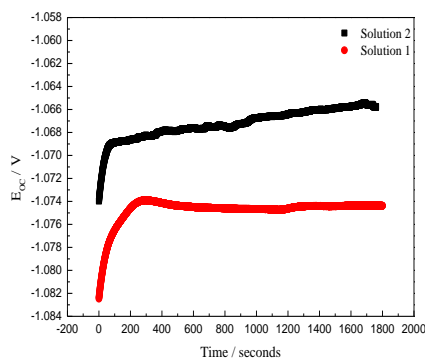


Figure 9. OCP vs. time curves of passivation process on substrates in different passivation solutions.

3.4.2. Effect of additives on morphology and composition of film during passivation

Fig. 10 depicts the surface morphologies of the passive film prepared in solution 2 at different passivation times. As the duration increased, the grains crystal of obtained passive films became coarser and the gap between the grain boundaries became larger. After 180 s, the film became rougher as it was repeatedly formed and dissolved.

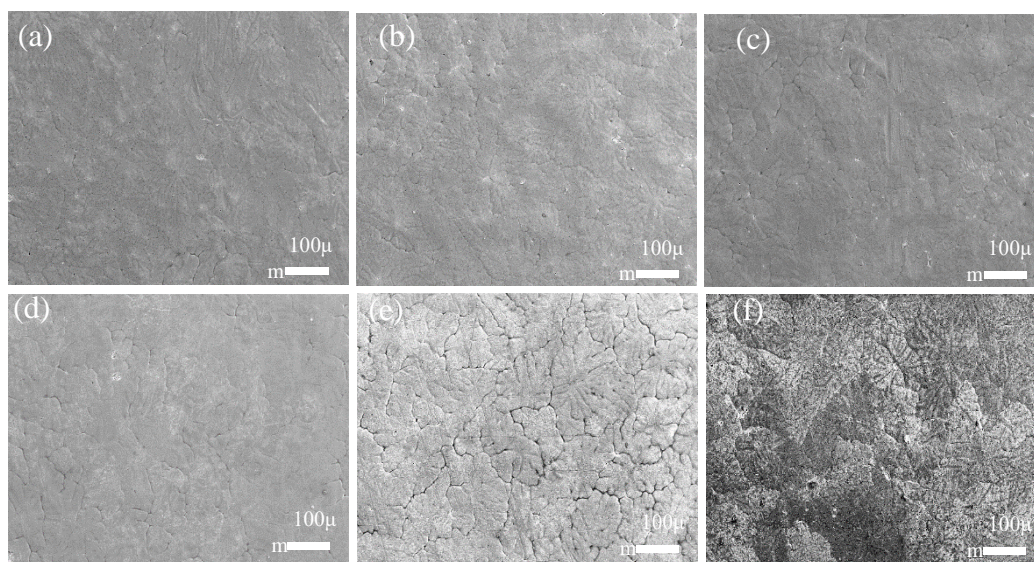


Figure 10. SEM morphology of surface of passive films prepared in solution 2 under different passivation times. (a) 30 s, (b) 60 s, (c) 120 s, (d) 180 s, (e) 240 s, and (f) 300 s.

When the passivation time was too long, the thickness of the generated passive film increased but corrosion resistance decreased. Therefore, suitable passivation time should range between 30 to 120 s. This inference could also be seen from the OCP vs. time curves measurements in solution 2 (shown in Fig. 9).

The main elements of the passive film prepared in solution 2 at different times are listed in Table 6. The contents of Zn decreased as time increased while those of O, Mo, P and V increased with time.

The contents of Si remained basically unchanged. Hence, inorganic substances such as molybdate, phosphate, and vanadate reacted continuously with zinc coating to deposit the reaction products on the surface and increase thickness of the passive film. The organic additives like silane and silica sol did not react with zinc layer but were adsorbed at the interface between the film and passivation solution to finally concentrate on the upper surface of the film.

Table 6. Contents of main forming-film elements under different passivation times in solution 2 (mass %).

Element	30s	60s	120s	180s	240s	300s
Zn	55.25	54.33	52.46	48.41	45.78	43.14
O	21.67	22.72	23.96	25.36	26.87	28.27
Mo	1.81	1.96	2.15	2.83	3.22	3.61
P	1.36	1.83	2.53	3.65	4.53	5.23
V	0.03	0.06	0.08	0.11	0.19	0.21
Si	0.63	0.62	0.65	0.60	0.65	0.62

4. CONCLUSIONS

The effects of organic additives on the performance and formation process of the passive film were investigated by accelerated corrosion testing, surface contact angle measurements, electrochemical testing, scanning electron microscopy, and energy dispersive X-ray spectroscopy. The following conclusions can be drawn:

- (1) The addition of organic substance into inorganic-based passivation solution greatly enhanced the comprehensive performance of the passive film.
- (2) The NSST results show increase by about 30% in salt-fog resistance of passivation-treated sample due to presence of organics.
- (3) The contact angle measurements revealed that organic-addition can increase the angle value of the obtained passive film by about 80%, leading to enhanced resistance to the corrosive medium.
- (4) The electrochemical performance results show that addition of organic additives reduced the corrosion of acquired passive film in 3.5% NaCl solution while optimizing the passivation process of substrate in the passivation solution and enhancing the film-forming effect.
- (5) The organic additives may have filled in the surface defects of generated passive films, such as gaps, cracks and pits, but did not react with zinc coating and instead concentrated on the film's surface.

In summary, the investigated inorganic-based passivation technology with addition of little amounts specific organic additives could effectively overcome the process limitations of batch hot-dip galvanization and yield excellent passive films, providing a promising future green manufacturing technique.

References

1. T. Peng, R. Man, *J. Rare Earths*, 27 (2009) 159.

2. G. Kong, J. T. Lu, H. J. Wu, *Journal Of Rare Earths*, 27 (2009) 164.
3. S.L. Manchet, J. Landoulsi, C. Richard, D. Verchere, *Surf. Coat. Technol.*, 205 (2010) 475.
4. J. Gou, G. Wang, Y. Ning, L. Guan, Y. Zhang, J. Liao and Y. Wang, *Surf. Coat. Technol.*, 366 (2019) 1.
5. G. Kong, J. Lu, S. Zhang, C. Che, H. Wu, *Surf. Coat. Technol.*, 205 (2010) 545.
6. Q. Liu, R. Ma, A. Du, X. Zhang, H. Yang, Y. Fan, X. Zhao and X. Cao, *Appl. Surf. Sci.*, 480 (2019) 646.
7. U. Bexell, T.M. Grehk, *Appl. Surf. Sci.*, 201 (2007) 4734.
8. H. Yang, X. Kong, W. Lu, Y. Liu, J. Guo and S. Liu, *Prog. Org. Coat.*, 67 (2010) 375.
9. Q. Li, H. Lu, J. Cui, M. An, D. Li, *Surf. Coat. Technol.*, 324 (2017) 146.
10. D. Lai, G. Kong, X. Xiao, C. Che, *Int. J. Electrochem. Sci.*, 13 (2018) 4055.
11. L. Jiang, M. Wolpers, P. Volovitch, K. Ogle, *Surf. Coat. Technol.*, 206 (2012) 3151.
12. W. Xu, L. Wei, Z. Zhang, Y. Liu, K.C. Chou, H. Fan, Q. Li, *J. Alloys Compd.*, 784 (2019) 859.
13. S.A. Abdel-Gawad, M.A. Sadik, M.A. Shoeib, *Int. J. Electrochem. Sci.*, 13 (2018) 2688.
14. F. Deflorian, M. Fedel, S. Rossi, P. Kamarchik, *Electrochim. Acta*, 56 (2011) 7833.
15. C.Y. Tsai, J.S. Liu, P.L. Chen, C.S. Lin, *Corros. Sci.*, 52 (2010) 3385.
16. H.E. Mohammadloo, A.A. Sarabi, *Appl. Surf. Sci.*, 387 (2016) 252.
17. L. Fachikov, D. Ivanova, *Appl. Surf. Sci.*, 258 (2012) 10160.
18. C.Y. Tsai, J.S. Liu, P.L. Chen, C.S. Lin, *Surf. Coat. Technol.*, 205 (2011) 5124.
19. R. Berger, U. Bexell, T.M. Grehk, S.E. Hornstrom, *Surf. Coat. Technol.*, 202 (2007) 391.
20. F. Deflorian, S. Rossi, L. Fedrizzi, P.L. Bonora, *Prog. Org. Coat.*, 52 (2005) 271.
21. Y. Hamlaoui, L. Tifouti, F. Pedraza, *Corros. Sci.*, 51 (2009) 2455.
22. D. Liu, Z. Yang, Z. Wang, C. Zhang, *Surf. Coat. Technol.*, 205 (2010) 2328.
23. Q. Liu, R. Ma, A. Du, X. Zhang, Y. Fan, X. Zhao, S. Zhang, X. Cao, *Corros. Sci.*, 150 (2019) 64.
24. S.J. Garcia, T.A. Markley, J.M.C. Mol, A.E. Hughes, *Corros. Sci.*, 69 (2013) 346.
25. M. Yuan, J. Lu, G. Kong, C. Che, *Surf. Coat. Technol.*, 205 (2011) 4507.
26. H.A. Sorkhabi, M.R. Majidi, K. Seyyedi, *Appl. Surf. Sci.*, 225 (2004) 176.
27. L. Zhang, S. Yang, H. Wu, X. Jie, *Int. J. Electrochem. Sci.*, 13 (2018) 3799.
28. X. Jiang, C. Lai, Z. Xiang, Y. Yang, B. Tan, Z. Long, L. Liu, Y. Gu, W. Yang, X. Chen, *Int. J. Electrochem. Sci.*, 13 (2018) 3224.
29. C.M. Fernandes, L.X. Alvarez, N.E.D. Santos, A.C.M. Barrios, E.A. Ponzio, *Corros. Sci.*, 149 (2019) 185.
30. K.S. Aneia, S. Bohm, A.S. Khanna, H.L.M. Bohm, *Nanoscale*, 42 (2015) 17879.
31. I. Santana, A. Pepe, E.J. Pique, S. Pellice, I. Milosev, S. Cere, *Surf. Coat. Technol.*, 265 (2015) 106.
32. A.C. Bastos, M.G.S. Ferreira, A.M. Simoes, *Prog. Org. Coat.*, 52 (2005) 339.
33. K.A. Yasakau, M.L.B. Zheludkevich, O.V. Karavai, M.G.S. Ferreira, *Prog. Org. Coat.*, 63 (2008) 352.
34. H. Zheng, Y. Shao, Y. Wang, G. Meng, B. Liu, *Corros. Sci.*, 123 (2017) 267.
35. B. Nikpour, B. Ramezanzadeh, G. Bahlakeh etc. , *Corros. Sci.*, 127 (2017) 240
36. B. Ramezanzadeh, Z. Haeri, M. Ramezanzadeh, *Chem. Eng. J.*, 303 (2016) 511.
37. Y. Xue, S. Wang, G. Zhao, A. Taleb, Y. Jin, *Surf. Coat. Technol.*, 363 (2019) 352.
38. R.M. Bandeira, J.V. Drunen, A.C. Garcia, G.T. Filho, *Electrochim. Acta*, 240 (2017) 215.
39. Y. Wu, P. Guo, Y. Zhao, X. Liu, Z. Du, *Prog. Org. Coat.*, 127 (2019) 231.
40. F.E. Heakal, A. Fekry, M.Z. Fatayerji, *Electrochim. Acta*, 54 (2009) 1545.
41. H. Gao, Q. Li, F. Chen, Y. Dai, F. Luo, L. Li, *Corros. Sci.*, 53 (2011) 1401.
42. F.E. Heakal, A.A. Ghoneim, A.M. Fekry, *J. Appl. Electrochem.*, 37 (2007) 405.